PROCEEDINGS OF SCIENCE

First measurements from charmless B decays at Belle II

Yun-Tsung Lai[a,*]

[a] *Kavli IPMU,*
5-1-5 Kashiwanoha, Kashiwa, Chiba, Japan
On behalf of the Belle II Collaboration

E-mail: yun-tsung.lai@ipmu.jp

We report on the first measurements of branching fractions, CP-violating charge-asymmetries, and polarizations in various charmless B decays at Belle II. We use a data sample of electron-positron collisions collected in 2019–2020 at the $\Upsilon(4S)$ resonance from the SuperKEKB collider. The data sample corresponds to an integrated luminosity of 34.6 fb^{-1}. All results are consistent with known values. In addition, these results provide extensive validations of the detector performance and analysis strategies.

BEAUTY2020
21-24 September 2020
Kashiwa, Japan (online)

*Speaker

PoS(BEAUTY2020)011

1. Introduction

Charmless B decays are important to search for non-Standard-Model (non-SM) physics in the flavor sector. Many decay channels are governed by 'penguin' amplitudes, which are sensitive to non-SM contributions within the loop. Studying them in detail is an important goal of the Belle II experiment [1]. With the largest sample of e^+e^- collisions anticipated in the next decade, Belle II is expected to improve significantly the measurements associated with charmless B decay, such as the determination of the CKM phase α/ϕ_2 [1, 2], the precision test of the $K\pi$ isospin sum rule [1, 3], and the study of local CP-violating asymmetries in the phase space of three-body B decays [1]. In addition, the measurement of decay-time-dependent CP violation in the penguin-dominated $B^0 \to \phi K^0$ mode, compared with corresponding results from $B^0 \to J/\psi K^0$ decays, will offer a probe of non-SM physics [1]. Measurements of the longitudinal-polarization fractions (f_L) of decays of B mesons into pairs of vector mesons also probe non-SM dynamics. Previous measurements of f_L with $B^0 \to J/\psi K^0$ decays showed a sizable contribution from transverse polarization, while most predictions expect the longitudinal component to dominate [4]. More precise f_L measurements may shed light on the issue.

SuperKEKB [5] is an asymmetric e^+e^+ collider, which started collision operations with the Belle II detector [6] in March 2019. We use a data sample of 34.6 fb^{-1}, which was collected at the $\Upsilon(4S)$ resonance up to May 2020. This report presents the measurements of branching fractions ($\mathcal{B}$), CP-violating charge-asymmetries ($\mathcal{A}_{\rm CP}$), and f_L based on the following B decays reconstructed in Belle II data: $B^0 \to K^+\pi^-$, $B^0 \to \pi^+\pi^-$, $B^+ \to K^+\pi^0$, $B^+ \to \pi^+\pi^0$, $B^+ \to K^0\pi^+$, $B^0 \to K^0\pi^0$, $B^+ \to K^+K^-K^+$, $B^+ \to K^+\pi^-\pi^+$, $B^0 \to \phi K^0$, $B^+ \to \phi K^+$, $B^0 \to \phi K^{*0}$, and $B^{*+} \to \phi K^{*+}$ [7, 8].

The B reconstruction, event-seletion criteria, and background suppression strategy are studied with various simulated signal and background samples. Charged-particle trajectories (tracks) are identified with inner vertex detectors and a central drift chamber with requirements on the displacement from the interaction point to reduce beam-background-induced tracks. The identification of charged particles uses the information from two particle-identification (PID) devices, a time-of-propagation counter in the barrel region and a proximity-focusing aerogel ring-image Cherenkov counter in the forward endcap region. Decays of π^0 candidates are reconstructed by combining two isolated clusters in the electromagnetic calorimeter, with requirements on the helicity angle and the results of a kinematic-fit constrained to the π^0 mass. Decays of K^0_S candidates are reconstructed from two opposite-charge pion candidates consistent with arising from a common vertex, with additional requirements on their kinematic and topological variables, e.g., momentum, flight distance, distance between pion trajectories, to further reduce the combinatorial background. Decays of ϕ candidates are reconstructed from two opposite-charge kaon candidates. Decays of K^{*0} candidates are reconstructed from one K^+ and one π^-, and decays of K^{*+} candidates are reconstructed from one K^0_S and one π^+. In three-body decays, we suppress the relevant peaking backgrounds from charmed or charmonium intermediate states by excluding the corresponding two-body mass ranges.

We use the following two variables to distinguish the signal B events from other backgrounds: the energy difference $\Delta E \equiv E^*_B - \sqrt{s}/2$ between the reconstructed B candidate and half of the collision energy in the $\Upsilon(4S)$ frame, and the beam-energy-constrained mass $M_{\rm bc} \equiv \sqrt{s/(4c^2) - (p^*_B/c)^2}$, where $\sqrt{s}$ is the collision energy, and E^*_B and p^*_B are the energy and momentum of reconstructed B candidates in the $\Upsilon(4S)$ frame.

2. Continuum background suppression

One of the main challenges of reconstructing charmless B decays is the large combinatorial background from $e^+e^- \to q\overline{q}$ ($q = u, d, s, c$) processes. Signal rates 10^5 times smaller than those to produce continuum background and the lack of distinctive final-state features (leptons or intermediate resonances) make the reconstruction of signal hard. Therefore, to discriminate between signal and continuum background, a binary boosted decision-tree (BDT) classifier is used which makes use of a non-linear combination of more than 30 variables. The input variables to the BDT include event topology variables, flavor-tagging information, vertex-fitting information, and kinematic-fit information. All of these variables are required to have little or no correlation with ΔE and $M_{\rm bc}$.

3. Signal extraction and measurement results

We use unbinned maximum likelihood fits to extract signal yields from the data to calculate various physics observables. In the $B \to hh$ and $B \to hhh$ ($h = K$ or π) analyses, only ΔE is fit for events restricted to $M_{\rm bc} > 5.27$ GeV/c^2. The fits to the two $B \to \phi K$ modes use five variables: ΔE, $M_{\rm bc}$, output of the continuum suppression BDT discriminator ($C'_{\rm out}$), K^+K^- candidate mass ($m_{K^+K^-}$), and cosine of the ϕ candidate's helicity angle ($\cos\theta_{H,\phi}$). The fits to the two $B \to \phi K^*$ modes use seven variables: $K^+\pi^-$ candidate mass ($m_{K\pi}$) and cosine of the K^* candidate's helicity angle ($\cos\theta_{H,K^*}$) in addition to those used in $B \to \phi K$ modes. By fitting the data, we determine the following quantities:

- Branching fractions: $\mathcal{B} = \frac{N}{\epsilon \times 2 \times N_{BB}}$, where N is the signal yield, ϵ is the signal reconstruction efficiency, which is determined from simulation and validated with control samples, and N_{BB} is the number of $B\overline{B}$ events (19.7×10^6 for B^+B^- and 18.7×10^6 for $B^0\overline{B}^0$). N_{BB} is obtained from the measured integrated luminosity, the exclusive $e^+e^- \to \Upsilon(4S)$ cross section, and $\mathcal{B}(\Upsilon(4S) \to B^0\overline{B}^0)$ [9].

- CP asymmetries: The raw asymmetries are obtained as $\mathcal{A} = \frac{N(b)-N(\overline{b})}{N(b)+N(\overline{b})}$, where $N(b)$ and $N(\overline{b})$ are the yields of the final-state mesons containing b and $\overline{b}$ flavors, respectively. The CP asymmetry $\mathcal{A}_{\rm CP}$ is obtained by subtracting the instrumental asymmetry $\mathcal{A}_{\rm det}$ from $\mathcal{A}$, where $\mathcal{A}_{\rm det}(K^+\pi^-) = -0.010 \pm 0.003$ and $\mathcal{A}_{\rm det}(K^0_S\pi^+) = -0.007 \pm 0.022$ are measured on large samples of $D^0 \to K^-\pi^+$ and $D^+ \to K^0_S\pi^+$ decays with negligible CP violation. Then $\mathcal{A}_{\rm det}(K^+)$ is determined as $\mathcal{A}_{\rm det}(K^+) = \mathcal{A}_{\rm det}(K^+\pi^-) - \mathcal{A}_{\rm det}(K^0_S\pi^+) + \mathcal{A}_{\rm det}(K^0_S) = -0.015 \pm 0.022$, where an upper bound on $\mathcal{A}_{\rm det}(K^0_S)$ is used based on the previous measurements [10].

- Longitudinal polarization fractions: $f_L = \frac{N_L/\epsilon_L}{N_L/\epsilon_L + N_T/\epsilon_T}$, where $N_{L(T)}$ and $\epsilon_{L(T)}$ are the signal yield and signal reconstruction efficiency with longitudinal (transverse) polarization, respectively. The distinctive helicity-angle distributions allow the separation of the two signal components.

Figures 1 and 2 show the ΔE distributions in data for $B^0 \to K^+\pi^-$ and $B^+ \to K^+K^-K^+$, with fit projections overlaid. Figure 3 shows the ΔE, $M_{\rm bc}$, $C'_{\rm out}$, $m_{K^+K^-}$, and $\cos\theta_{H,\phi}$ distributions in data

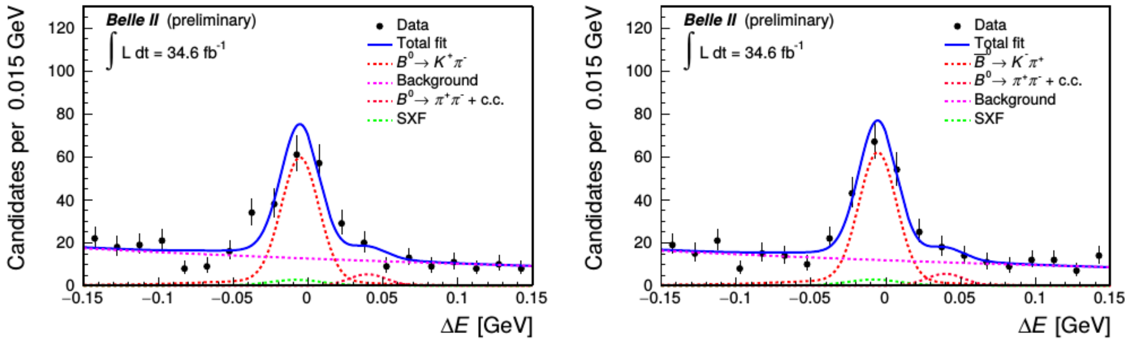

Figure 1: Distribution of ΔE for $B^0 \to K^+\pi^-$ (left) and $\overline{B}^0 \to K^-\pi^+$ (right) decays with fit projections overlaid.

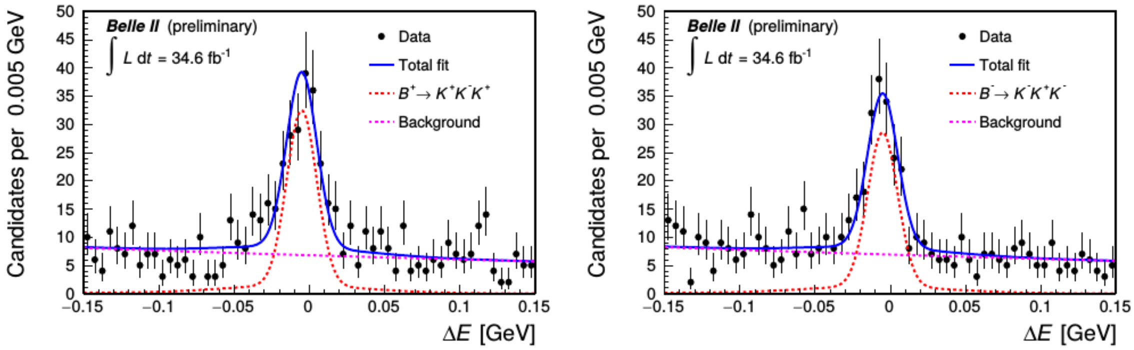

Figure 2: Distribution of ΔE for $B^+ \to K^+K^-K^+$ (left) and $B^- \to K^-K^+K^-$ (right) decays with fit projections overlaid.

for $B^+ \to \phi K^+$, with fit projections overlaid. Figure 4 shows the ΔE, $M_{\rm bc}$, $C'_{\rm out}$, $m_{K^+K^-}$, $\cos\theta_{H,\phi}$, $m_{K\pi}$, and $\cos\theta_{H,K^*}$ distributions in data for $B^+ \to \phi K^{*+}$ decay, with fit projections overlaid. The major systematic uncertainties come from tracking, PID, and fit modelling. All the measurement results are summarized in Table 1.

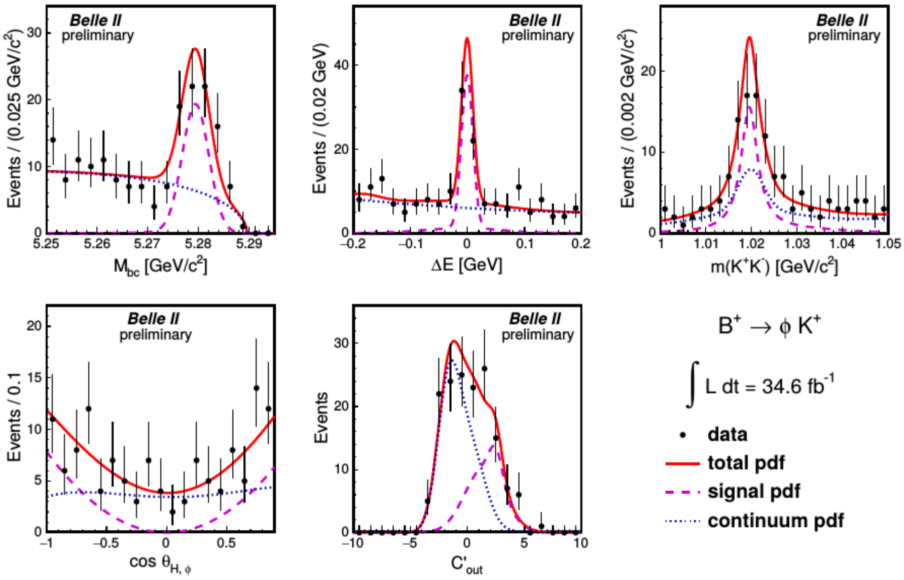

Figure 3: Distribution of ΔE, $M_{\rm bc}$, $C'_{\rm out}$, $m_{K^+K^-}$, and $\cos\theta_{H,\phi}$ for $B^+ \to \phi K^+$ decay with fit projections overlaid.

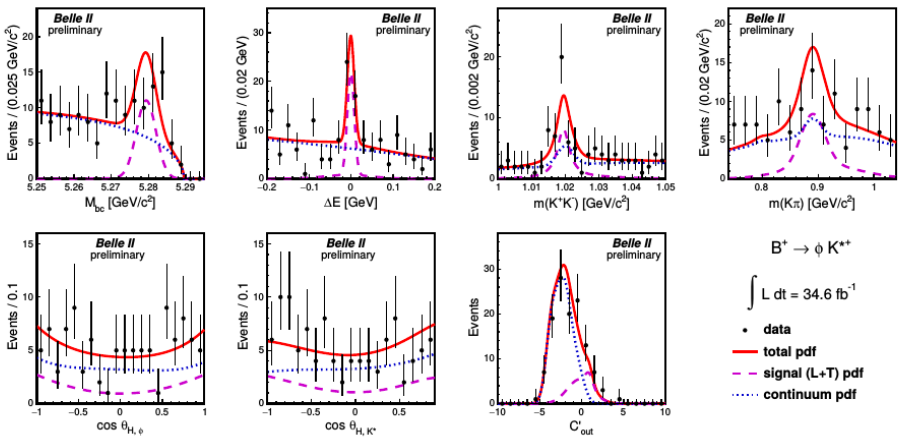

Figure 4: Distribution of ΔE, $M_{\rm bc}$, $C'_{\rm out}$, $m_{K^+K^-}$, $\cos\theta_{H,\phi}$, $m_{K\pi}$, and $\cos\theta_{H,K^*}$ for $B^+ \to \phi K^{*+}$ decay with fit projections overlaid.

Table 1: Summary of measurement results. The first uncertainties are statistical and the second ones are systematic.

Mode	$\mathcal{B}$ (10^{-6})	$\mathcal{A}_{\rm CP}$	f_L
$B^0 \to K^+\pi^-$	$18.9 \pm 1.4 \pm 1.0$	$0.030 \pm 0.064 \pm 0.008$	-
$B^0 \to \pi^+\pi^-$	$5.6^{+1.0}_{-0.9} \pm 0.3$	-	-
$B^+ \to K^+\pi^0$	$12.7^{+2.2}_{-2.1} \pm 1.1$	$0.052^{+0.121}_{-0.119} \pm 0.022$	-
$B^+ \to \pi^+\pi^0$	$5.7 \pm 2.3 \pm 0.5$	$-0.268^{+0.249}_{-0.322} \pm 0.123$	-
$B^+ \to K^0\pi^+$	$21.8^{+3.3}_{-3.0} \pm 2.9$	$-0.072^{+0.109}_{-0.114} \pm 0.024$	-
$B^0 \to K^0\pi^0$	$10.9^{+2.9}_{-2.6} \pm 1.6$	-	-
$B^+ \to K^+K^-K^+$	$32.0 \pm 2.2 \pm 1.4$	$-0.049 \pm 0.063 \pm 0.022$	-
$B^+ \to K^+\pi^-\pi^+$	$48.0 \pm 3.8 \pm 3.3$	$-0.063 \pm 0.081 \pm 0.023$	-
$B^0 \to \phi K^0$	$5.9 \pm 1.8 \pm 0.7$	-	-
$B^+ \to \phi K^+$	$6.7 \pm 1.1 \pm 0.5$	-	-
$B^0 \to \phi K^{*0}$	$11.0 \pm 2.1 \pm 1.1$	-	$0.57 \pm 0.20 \pm 0.04$
$B^{*+} \to \phi K^{*+}$	$21.7 \pm 4.6 \pm 1.9$	-	$0.58 \pm 0.23 \pm 0.02$

4. Summary

Belle II reports its first measurements of charmless B decays with a data sample corresponding to 34.6 fb^{-1}. The measurements include branching fractions, CP asymmetries, and longitudinal polarization fractions. All the results are in agreement with the known values, and provide a good validation of the detector performance and analysis strategies.

References

[1] E. Kou *et al.* (Belle II Collaboration), PTEP **2019** (2019) no.12, 123C01, arXiv:1808.10567 [hep-ex].

[2] M. Gronau and D. London, Phys. Rev. Lett. **65** (1990) 3381 .

[3] M. Gronau, Phys. Lett. B **627** (2005) no. 1, 82-88.

[4] M. Tanabashi *et al.* (Particle Data Group), Phys. Rev. D **98** (2018) 030001.

[5] K. Akai *et al.*, Nucl. Instrum. Meth. A **907** (2018) 188-199 .

[6] T. Abe *et al.* (Belle II Collaboration), arXiv:1011.0352 [hep-ex].

[7] F. Abudinén *et al.* (Belle II Collaboration), arXiv:2009.09452 [hep-ex].

[8] F. Abudinén *et al.* (Belle II Collaboration), arXiv:2008.03873 [hep-ex].

[9] A. J. Bevan *et al.* (Belle and BaBar Collaborations), Eur. Phys. J. **C74** (2014) 3026, arXiv:1406.6311 [hep-ex].

[10] A. Davis *et al.* (LHCb Collaboration), [LHCb-PUB-2018-004].